Voltammetric study of triazole antifungal agent terconazole on sp3 and sp2 carbon-based electrode materials

Jan Fischer, Javier González-Martín, Pawel Lochyński, Hana Dejmková, Karolina Schwarzová-Pecková, Marisol Vega

PII: S1572-6657(20)30237-X

DOI: https://doi.org/10.1016/j.jelechem.2020.114054

Reference: JEAC 114054

To appear in: *Journal of Electroanalytical Chemistry*

Received date: 9 December 2019

Revised date: 7 March 2020

Accepted date: 9 March 2020

Please cite this article as: J. Fischer, J. González-Martín, P. Lochyński, et al., Voltammetric study of triazole antifungal agent terconazole on sp3 and sp2 carbon-based electrode materials, *Journal of Electroanalytical Chemistry*(2020), https://doi.org/10.1016/j.jelechem.2020.114054

Voltammetric study of triazole antifungal agent terconazole on sp^3 and sp^2 carbon-based electrode materials

Jan Fischer [a], Javier González-Martín [a,b], Pawel Lochyński [c], Hana Dejmková [a], Karolina Schwarzová-Pecková [a], Marisol Vega [b,d]*

[a] *Charles University, Faculty of Science, Department of Analytical Chemistry, UNESCO Laboratory of Environmental Electrochemistry, Albertov 6, CZ-12843, Prague 2, Czech Republic*

[b] *University of Valladolid, Institute of Sustainable Processes, Dr. Mergelina s/n, 47011 Valladolid, Spain*

[c] *Wroclaw University of Environmental and Life Sciences, Institute of Environmental Engineering, Norwida 25, PL-50375 Wroclaw, Poland*

[d] *University of Valladolid, Department of Analytical Chemistry, Faculty of Science, Campus Miguel Delibes, Paseo de Belén 7, 47011 Valladolid, Spain, solvega@qa.uva.es*

Abstract

Terconazole belongs to synthetic triazole antifungal agents, inhibiting biosynthesis of ergosterol or other sterols and thus disrupting cell wall synthesis in fungi. In this study, electrochemical behaviour of terconazole was studied for the first time using cyclic voltammetry and differential pulse voltammetry on boron doped diamond electrode (BDD) with different surface treatments leading to O-terminated, H-terminated and polished surfaces, as well as on glassy carbon (GCE) and basal-plane pyrolytic graphite electrodes (PGE). Terconazole is not reducible within the potential window on these electrode materials. It is oxidizable in aqueous solutions in pH range from 2.0 to 12.0 in two steps due to the presence of piperazine ring in its molecule, possessing two redox centres at the tertiary nitrogen atoms, by an ECE mechanism. Optimal conditions were found for determination of terconazole in 0.1 mol L^{-1} phosphate buffer pH 7.2. Using differential pulse voltammetry, the lowest detection limit of 0.40 μmol L^{-1} and excellent repeatability (RSD 1.1 %) were achieved on O-terminated BDD when *in-situ* anodic activation was used prior to each scan. This is beneficial in comparison with GCE and PGE; their necessity of *ex-situ* polishing worsens the signal repeatability (RSD ~ 4%) and detection limits reaching 0.50 μmol L^{-1} and 1.23 μmol L^{-1}, respectively.

Keywords

Boron doped diamond electrode; Glassy carbon electrode; Pyrolytic graphite electrode; Surface termination; Terconazole; Voltammetry.

1. Introduction

Azoles are a group of chemicals used as pesticides or pharmaceuticals, acting as antifungal agents. The diazole (imidazole) or triazole rings are key building blocks of these compounds, modulating their biological activity, possibly together with other moieties included in their molecules such as piperazine heterocycle [1]. Azoles show selective inhibition of cytochrome P450 enzymes leading to disruption of the pathways of synthesis of ergosterol, an essential fungal sterol present in cell membranes [2]. Terconazole ((+-)-1-{4-[cis-2-(2,4-Dichlorophenyl)-2-(1H-1,2,4-triazol-1-ylmethyl)-1,3-dioxolan-4-ylmethoxy]phenyl}-4-isopropylpiperazine), possessing triazole and piperazine rings in its structure (Scheme 1), is used as antimycotic agent. It inhibits the activity of the cytochrome P450 14-alpha-demethylase in *Candida* species [3], which leads to the accumulation of lanosterol and other methylated sterols and the decrease in ergosterol concentration. Thus, it is used in suppositories and creams to treat vulvovaginal candidiasis. Both administration forms have demonstrated high levels of safety, efficacy, and tolerability in clinical trials [4]. It is a chiral drug, in praxis used as a racemic mixture. Nevertheless, pharmacological activity of individual enantiomers can be different, which leads to efforts on differentiation between them (only two enantiomers of terconazole exist because of the cis configuration of the 2,4-dichlorophenyl group and hydrogen at the two chiral centers) [5].

Several reports exist on determination of terconazole alone or in combination with other drugs and preservatives used in pharmaceutical preparations. A spectrophotometric method has been developed for determination of terconazole in dosage forms [6]. Simultaneous determination with the preservative benzoic acid was achieved using derivative spectrophotometry and high performance liquid chromatography with UV detection [7]. The latter methods and micellar liquid chromatography were used for determination of terconazole in dosage forms and human plasma [8]. Electrokinetic chromatography enables separation of the two enantiomers of terconazole [5]. Stability testing of terconazole, identification of impurities and characterization of products raised by forced degradation have been performed based on ultra-performance liquid chromatography coupled to time of flight tandem mass spectrometry (UPLC-Q-TOF/MS/MS) and NMR [9].

Concerning the electrochemistry of triazole and imidazole agents, literature data are rather scarce. Since the triazole moiety is not electrochemically active, a universal approach could be the utilization of complexation reactions with metal ions [10], *i.e.*, enhancement of voltammetric signals assigned to oxidation of a metallic electrode in the presence of the triazolic compound due to its complexation reaction [11, 12]. The direct redox activity of triazoles relies on other moieties, *e.g.*, electrochemical oxidation of the amino group in amitrole [13, 14] or reduction of azomethine moiety (*e.g.*, in propiconazole). The oxidizable piperazine moiety [15] enables voltammetric determination of azolic pharmaceuticals (*e.g.*, ketoconazole, posaconazole, itraconazole) [16-22]. It follows from Table 1, which summarizes the characteristics and limits of detection of the voltammetric methods that their oxidation occurs at potentials ranging from *ca* +0.5 V to +0.75 V on carbon-based electrodes, including boron doped diamond (BDD). This material offers advantageous properties for electroanalysis of organic compounds, including mechanical stability, low background current, wide potential window especially in the region of positive potentials and usually low adsorbability of reaction by-products and products resulting in fouling resistivity [23-25]. Its electrochemical properties are influenced by the surface pretreatment. While *in-situ* anodic electrochemical activation in the region of positive potentials leads to water oxidation and generation of $HO^{\bullet}$ radicals, and consequently to oxygen termination of the BDD surface (O-BDD) characterized by the presence of hydroxyl, carbonyl, ether, and carboxyl groups [26, 27], application of negative potential in the region of hydrogen evolution leads to hydrogen termination (H-BDD) [28]. The other activation approach is polishing of BDD surface by alumina (p-BDD), leading to loss of oxygen-containing groups, especially those bonded to sp^2 hybridized carbons at the surface [26]. Besides the triazole pharmaceuticals ketoconazole [22], BDD succeeded in oxidation of other compounds possessing piperazine moiety, *e.g.*, the anticancer drug imatinib [29] and fluoroquinolone antibiotic pefloxacin [30].

In this contribution, the electrochemical behaviour of terconazole has been investigated for the first time. A representative variety of sp^3 and sp^2 carbon-based electrodes was used for that purpose. Besides O-BDD, H-BDD, and p-BDD electrodes, glassy carbon electrode (GCE) and pyrolytic graphite electrode (PGE) were used to represent widely used sp^2 carbon electrode materials. Pyrolytic graphite is a heterogenous three-dimensional graphite material, composed of parallelly stacked sheets of graphene comprising flat basal planes and edge plane perpendicular to them. It has relatively wide potential window, surprisingly also in the region of negative potentials [31]. Glassy carbon comprises of randomly intertwined ribbons of graphitic planes, thus it is disordered, with higher interplanar

spacing in comparison to pyrolytic graphite [32]. Comparison of performance of these materials in electrooxidation of terconazole was made and its mechanism proposed. A differential pulse voltammetric (DPV) quantitation method based on oxidation signal of terconazole was optimized.

Table 1. Characteristics of polarographic and voltammetric methods for detection of azolic pharmaceuticals possessing piperazine moiety.

Compound	E_p [V]	Working electrode	Reference electrode	Technique	Supporting electrolyte	LOD [μmol L^{-1}]	Ref.
Itraconazole	−1.48	DME	Ag/AgCl	DPP	BRB, pH 7	0.1	[33]
Ketoconazole	−1.56	DME	Ag/AgCl	DPP	BRB, pH 7	0.50	[33]
Ketoconazole	−1.46	p-AgSAE	Ag/AgCl	SWV	BRB, pH 12	0.12	[34]
Ketoconazole	+0.54	GCE	Ag/AgCl	CV, AdS-DPV	NH_3-NH_4Cl, pH 9	0.00004	[18]
Ketoconazole	≈ +0.5	GCE	Pd	CV	PB, pH 3, 5, 7	--	[16]
Itraconazole	≈ +0.5	GCE	Pd	CV	PB, pH 3, 5, 7	--	[16]
Posaconazole	≈ +0.5	GCE	Pd	CV	PB, pH 3, 5, 7	--	[16]
Ketoconazole	≈ +0.6	GCE	SCE	CV, SWV	NH_3-NH_4Cl, pH 9	0.075	[19]
Ketoconazole	≈ +0.6	MWCNTs-GCE	SCE	CV, LSV, DPV	PB, pH 7	0.44	[20]
Ketoconazole	≈ +0.55	CPE	Ag/AgCl	AdS-DPV	PB, pH 12	0.024	[17]
Itraconazole	+0.66	CPE	Ag/AgCl	CV, AdS-DPV, AdS-SWV	BRB, pH 2	0.012	[21]
Itraconazole	+0.75	UTGE	Ag/AgCl	CV, AdS-DPV, AdS-SWV	BRB, pH 2	0.015	[21]
Itraconazole	+0.63	PCE	Ag/AgCl	CV, AdS-DPV, AdS-SWV	BRB, pH 2	0.013	[21]
Ketoconazole	+0.59	BDDE	SCE	SWV	NH_3-NH_4Cl, pH 9	0.083	[22]
Terconazole	≈ +0.50	O-BDDE; GCE, PGE	Ag/AgCl	CV, DPV	PB, pH 7.2	0.4; 0.5; 1.24	This study

CPE – carbon paste electrode; MWCNTs – multi-walled carbon nanotubes; PCE – pencil graphite electrode; p-AgSAE – polished silver solid amalgam electrode; UTGE – ultra-trace graphite electrode
AdS – adsorptive anodic stripping; DPV – differential pulse voltammetry; SWV – square wave voltammetry; BRB – Britton – Robinson buffer; PB – phosphate buffer

2. Experimental

2.1. Reagents and Solutions

Terconazole was purchased from Sigma-Aldrich (VETRANAL ™, analytical standard). The standard solution (c = $1 \cdot 10^{-3}$ mol L^{-1}) was prepared in deionized water. It was stored at room temperature in the dark. Piperazine (Sigma-Aldrich, analytical standard) stock solution (c = $1 \cdot 10^{-3}$ mol L^{-1}) was prepared in deionized water. Other chemicals utilized throughout the experiments were from Czech local producers and of analytical grade (if not specified otherwise). Britton – Robinson buffer was prepared by mixing 0.04 mol L^{-1} H_3PO_4, H_3BO_3 and CH_3COOH solution with an adequate amount of 0.2 mol L^{-1} NaOH, to reach the required pH in the range from 2.0 to 12.0. 0.1 mol L^{-1} phosphate buffer pH 2.3 was prepared by mixing H_3PO_4 and $NaH_2PO_4 \cdot 2H_2O$ solutions. 0.1 mol L^{-1} phosphate buffer pH 7.2 was prepared mixing $NaH_2PO_4 \cdot 2H_2O$ and $Na_2HPO_4 \cdot 12H_2O$ solutions. Borate buffer at pH 9.2 was prepared by precise addition of 0.2 mol L^{-1} NaOH to 0.1 mol L^{-1} H_3BO_3 solution. Deionized water was obtained from a Millipore Q-plus System (Millipore, USA).

2.2. Instrumentation

Computer-controlled Eco-Tribo Polarograph system with PolarPro version 5.1 software (EcoTrend Plus, Prague, Czech Republic) was used for voltammetric measurements. All measurements were performed in the three-electrode setup with Ag|AgCl (3 mol L^{-1} KCl) as a reference electrode and platinum wire as an auxiliary electrode (both from Elektrochemické detektory, Turnov, Czech Republic). The working electrodes were: BDD electrode (A = 12.6 mm^2, B/C= 10000 ppm when not specified otherwise, film thickness 3 μm; NeoCoat, Switzerland); basal oriented homemade PGE with square face surface area of A = 9 mm^2; glassy carbon disk electrode (A = 3.1 mm^2; Metrohm, Switzerland). The pH measurements were carried out by digital pH Meter 3510 (Jenway, UK) with combined glass electrode.

2.3. Procedures

The measured volume of supporting electrolyte and sample was 10 mL, unless otherwise specified. The surfaces of the electrodes were pretreated and activated between individual scans as follows: p-BDD – pretreated by polishing using Al_2O_3 (0.5 μm) suspension (Elektrochemické detektory, Turnov, Czech Republic) in deionized water for 5 min, followed by sonication in methanol and deionized water to remove the alumina residues. Activation prior each scan was performed by polishing using Al_2O_3 suspension for 30 s; O-BDD – a

pretreatment potential of +2.4 V was applied for 20 min in stirred 0.5 mol L^{-1} H_2SO_4 solution and 5 minutes in supporting electrolyte before each series of measurements. Anodic activation at +2.4 V for 5 s directly in measured solution was also applied between individual scans in optimized DPV procedure and in measurement of the scan rate dependence by cyclic voltammetry; H-BDD – a pretreatment potential of −2.4 V was applied for one hour in stirred 0.5 mol L^{-1} H_2SO_4 solution before all measurements, and 5 min before each series of measurement. Measurement in positive potential region was carefully performed within the potential window of H-BDD to prevent surface oxygenation and conversion to O-BDD. GCE was polished using Al_2O_3 suspension in deionized water for 30 s followed by rinsing with deionized water prior to each scan. The surface of PGE was dried after each scan and renewed using adhesive tape.

Unless otherwise stated, a scan rate of 20 mV s^{-1}, pulses with a duration of 80 ms and modulation amplitude ±50 mV were used in DPV. For CV, scan rate of 100 mV s^{-1} was set. Peak-current values (I_p) were evaluated from the line connecting current minima at both sides of the voltammetric peak. All the solutions were degassed by 5 min passing nitrogen, before measurements were performed.

The concentration dependences were constructed from the average of four replicate measurements for each concentration of terconazole and were evaluated by the least squares linear regression method. For differential pulse voltammetry, the limits of detection (L_D) were calculated as a threefold of the standard deviation *s* of the peak currents (ten runs) of the lowest measurable concentration, divided by the slope of corresponding calibration curve.

3. Results and discussion

3.1. Voltammetric studies of terconazole and characterization of its redox reactions

Firstly, cyclic voltammetry of 1 mmol L^{-1} $[Fe(CN)_6]^{3-/4-}$ redox couple recorded in 1 mol L^{-1} KCl at the scan rate of 0.1 mV s^{-1} was used for characterization of tested electrode surfaces. The peak potential difference ΔE_p between anodic and cathodic peaks of $[Fe(CN)_6]^{3-/4-}$ recorded on different BDD surfaces (O-BDD, H-BDD, and p-BDD), and further on PGE and GCE, were 410 ± 20 mV, 85 ± 10 mV, 90 ± 5 mV, 550 ± 25 mV, and 65 ± 4 mV, respectively. These values clearly indicate differences in chemical composition of moieties terminating tested surfaces, as it is known that oxygen containing groups with π-electrons inhibit electron transfer of this redox marker [32].

Then, cyclic voltammetry was used as the first-choice technique to characterize the electrochemical behavior of terconazole on different BDD surfaces (O-BDD, H-BDD, and p-BDD), PGE and GCE in acidic (phosphate buffer pH 2.3), neutral (phosphate buffer pH 7.2), and alkaline (borate buffer pH 9.3) media. CVs recorded in anodic direction are depicted in Fig. 1. The main oxidation signal at potentials ranging from *ca* +0.55 V to +0.90 V (depending on the electrode material) is observable on all electrodes and in all electrolytes tested and it shifts slightly to less positive values with increasing pH. This indicates that the redox-active group is in acid-base equilibrium and the proton transfer precedes the electron transfer rate-determining step. This oxidation step is irreversible in all instances with the exception of acidic media on PGE and H-BDD, where a quasireversible process was observed with ΔE_p of 0.1 V and 0.09 V, respectively. Such behavior was previously observed also for ketoconazole [22]. It can be ascribed to the electron uptake from piperazine moiety leading to the formation of radical cation at the proximal nitrogen (aminium radical cation), and fast reverse cathodic reaction. For both ketoconazole and terconazole, this quasireversible behavior was observed only in acidic media and on relatively hydrophobic surfaces (for details see further Scheme 1 and attached description of oxidation mechanism of terconazole). When comparing peak potentials E_p for the mentioned electrode materials, no substantial differences can be traced, confirming similar interaction of terconazole and its oxidation byproducts with the mentioned surfaces and similar kinetics of electron transfer. It is important in the view of other studies, where substantial differences in positioning of anodic/cathodic signals were reported when comparing BDD with other carbon-based electrodes [23, 35, 36] or when comparing O-, H- and polished BDD surfaces, with the O-terminated one, observed to inhibit electron transfer and thus shifting anodic/cathodic signals to more positive/negative potentials [37].

The second peak appearing at more positive potentials at *ca* +1.0 V – + 1.25 V is well observable on O-BDD and p-BDD in all media and on H-BDD in acidic media. On the other hand, it is absent on CVs recorded on the sp^2 carbon electrode materials due to its low intensity or narrower potential windows of the latter electrodes. Nevertheless, it can be visualized on all electrode materials using differential pulse voltammetry. DP voltammograms of $1 \cdot 10^{-4}$ mol L^{-1} terconazole on O-BDD, GCE and PGE at different pH values are presented in Fig. 2 and the corresponding peak potential E_p *vs.* pH dependences are depicted in Fig. 3. For the first anodic signal, the linearity of these dependences is described by the following equations (1-3) for O-BDD, GCE, and PGE, respectively, in pH range 4.0 –12.0:

$E_{p,O\text{-}BDD}$ (mV) = −25.1 pH + 776 (R^2 = 0.991) (1)

$E_{p,GCE}$ (mV) = −25.6 pH + 815 (R^2 = 0.975) (2)

$E_{p,PGE}$ (mV) = −24.8 pH + 803 (R^2 = 0.984) (3)

The slopes of about 25 mV per pH unit suggest a redox process where two electrons are exchanged per one proton [38].

For further experiments and investigation of the mechanism of electrochemical oxidation of terconazole, 0.1 mol L^{-1} phosphate buffer pH 7.2 was chosen, where well developed anodic signals were obtained on all tested electrode materials. Further, this neutral medium is compatible with conditions required in physiological studies, *e.g.* for evaluation of enzyme activity in the presence of triazole agents. H-BDD and p-BDD were excluded from further studies, because their unintended conversion to O-BDD occurs easily when exposed to highly positive potentials in the region of water decomposition reaction, being close to oxidation signals of terconazole. Reverse conversion to H-BDD surface requires time-demanding re-hydrogenation using highly negative potentials or negative current densities, or polishing to obtain p-BDD, both performed *ex-situ*. Thus, from practical reasons, *in-situ* anodic activation leading to O-BDD was chosen. The scan rate dependences of the first anodic signals were evaluated on O-BDD, GCE and PGE and can be characterized by the following equations (4-6, respectively) for scan rate range 5 – 200 mV s^{-1}:

$I_{p,O\text{-}BDD}$ (μA) = 0.866 $v^{1/2}$ (mV s^{-1}) – 0.702 (R^2 = 0.9993) (4)

$I_{p,GCE}$ (μA) = 0.790 $v^{1/2}$ (mV s^{-1}) – 1.521 (R^2 = 0.9753) (5)

$I_{p,PGE}$ (μA) = 0.865 $v^{1/2}$ (mV s^{-1}) – 0.403 (R^2 = 0.9977) (6)

The values of I_p obviously increase linearly with square root of the scan rate, which is common behavior for diffusion-controlled electrochemical reactions. Diffusion-controlled mechanism can be also verified by representing logarithm of peak current versus logarithm of the scan rate. Theoretical slope of 0.5 for the linear dependence should be achieved for a diffusion-controlled electrode reaction. The obtained slope values were 0.561, 0.447, and 0.709 for O-BDD, GCE, and PGE, respectively, and intercepts 0.223, 0.059, and 0.642 were different from 0. Thus, it was not possible to assure that the process is completely diffusion-controlled. It seems to be the main mechanism controlling the processes at O-BDD and GCE; in contrast, for PGE a more significant adsorptive contribution can be expected. The flat basal planes of PGE are better suited for adsorption of terconazole molecule possessing three flat aromatic rings than randomly oriented sp^2/sp^3 carbon structures in GCE and BDD.

The number of exchanged electrons n and the anodic charge transfer coefficient α_a were calculated from the slope b of the plot of peak potential E_p vs. natural logarithm of the

scan rate *v* evaluated from cyclic voltammograms measured in phosphate buffer pH 7.2, using the equation (eq. 7) derived for diffusion-controlled anodic processes [39]:

$$b = \frac{RT}{2\alpha_a n\mathbf{F}} \qquad (7)$$

where *F*, *R*, and *T* are Faraday constant, molar gas constant, and temperature, respectively. Based on eq. 7, $\alpha_a n$ values were evaluated to be 0.911, 0.946, and 0.930 for O-BDD, GCE, and PGE, respectively. According to IUPAC recommendation [39], the values of $\alpha_a n$ close to one should be interpreted as a reversible release or uptake of the first transferred electron followed by a rate-determining chemical step, since the simultaneous release or uptake of two electrons is highly improbable. Taking this assumption into account, the transfer coefficient α_a for anodic process should be calculated as (eq. 8):

$$\alpha_a = \frac{RT}{\mathbf{F}}\left(\frac{\boldsymbol{d}\ln|j_a|}{\boldsymbol{d}E}\right) \qquad (8)$$

where j_a symbolizes the anodic current density. The resulting α_a values are equal to 0.97, 1.04 and 0.94 for O-BDD, GCE, and PGE, *i.e.*, approaching the value of one for reversible processes and confirming the legitimacy of the described approach. From the above mentioned E_p *vs.* pH dependences (eq. 1-3) and respecting results based on eq. 7 and 8, it can be concluded that terconazole is oxidized by ECE mechanism with two electrons and one proton exchange. The oxidation is initialized by one electron transfer followed by a slow rate-determining chemical step, followed by a second one electron process.

To transfer this cognition to the mechanism of electrooxidation of terconazole, its acid-base properties and potential redox-active sites must be jointly evaluated. The piperazine ring is a clear target of electrooxidation in the structure of terconazole, as this heterocycle possesses electrons in lone electron pairs on nitrogen atoms and its oxidation has been described for a number of other compounds possessing this moiety on BDD [29, 30] and other electrode materials [15, 16, 40-43]. The suggested mechanisms discuss a sequence of electrochemical and chemical ((de)protonation) reaction steps with respect to the structure motifs conjugated to both nitrogen atoms of the piperazine moiety and their pK_a values (pK_a values of corresponding conjugated acids). Nevertheless, comparison of electrochemical oxidation/reduction mechanism of piperazine itself with the more complex compounds possessing the piperazine ring is not reasonable, because the groups attached to the piperazine nitrogens significantly change their basicity and redox behavior, as the secondary amines undergo redox processes different from those of tertiary amines attached to alkyl or aromatic moieties. The pK_a values of piperazine are 9.73 and 5.33 [44, 45] and its electrochemical oxidation/reduction behavior on p-BDD electrode is obvious from Fig. S1 (in the

Supplemental material). This electrode material, differential pulse voltammetry, and phosphate buffer pH 7.4 were used to visualize the signals, as these were rather indistinctive using different conditions and cyclic voltammetry. While the oxidation signal of piperazine is placed at +0.79 V, its reduction proceeds at −0.67 V. Oxidation/reduction potentials for selected azole agents summarized in Table 1 reveal significant shift from these values, indicating change in their reaction mechanism. Regarding oxidation of the piperazine containing azole compounds, usually lower E_p values are detected, compared to those observed for free piperazine. Moreover, two anodic signals have frequently been reported [41]. Further, simple substituted piperazines exhibit lower pK_a and thus lower basicity, more pronounced for tertiary than for secondary amines [45]. The reasonable calculated pK_a value for terconazole, available in the literature, was 8.8 [46] (referring to conjugated acid of the distal (from the benzene ring) nitrogen of the piperazine ring, see Scheme 1). Other two published pK_a values ($pK_{a1,2}$ < 1.5) [47] are given without specification; they should characterize the acidity of the conjugated acid of proximal nitrogen of the piperazine ring and the triazole moiety. Nevertheless, these values seem to be lower than expected values, in view of pK_a values of structurally similar triazoles possessing piperazine nitrogen bonded to benzene ring, *e.g.*, itraconazole (pK_a = 3.7) [16], posaconazole (pK_a = 3.6) [48], and ketoconazole (pK_a = 2.94) [49], where acidity of the proximal protonated nitrogen in piperazine ring conjugated to an aromatic ring is increased due to the inductive effect of proximal amide. The N2 in 1,2,4-triazole has the pK_a of 2.2 (conjugated acid) [50].

The E_p *vs.* pH dependences for the main oxidation signal of terconazole on O-BDD, PGE and GCE described in Eq. (1 – 3) are linear in a wide pH range (4 – 12) thus suggesting the proximal nitrogen of the piperazine ring, non-protonated in the pH range studied, to be oxidized. This is in agreement with data from other studies on structurally similar compounds with piperazine ring possessing tertiary amines attached to an aliphatic chain on one nitrogen atom and an aromatic ring on the other nitrogen, *e.g.*, trazodone [40, 41], nefazodone [43] or quetiapine [51]. The suggested oxidation mechanism for terconazole **1** is given in Scheme 1 and can be regarded as ECE reaction pathway. It involves one-electron transfer from the proximal nitrogen, which gives rise to a radical cation (aminium radical cation **2**). It stabilizes through deprotonation (chemical reaction step) and another one electron oxidation to form a quarternary Schiff base (protonated imine **3**). The deprotonation is inhibited in acidic media, thus stability of the aminium radical cation **2** is increased and its fast reverse reduction to terconazole **1** gives rise to quasireversible redox pair on PGE and H-BDD (see Fig. 1B, E). The consequent hydrolysis leads to cleavage of the protonated imine **3** so that acetone **4** and

secondary amine on the piperazine ring **5** are the final products. Obviously, the suggested mechanism with shift of redox active sites from the proximal to the distal nitrogen of piperazine moiety for the first and second electron transfer, respectively, excludes simultaneous release of both electrons, thus substantiating the use of eq. 7 and 8 for calculation of α_a according to IUPAC recommendation [39].

The second oxidation signal is rather indistinctive, better developed only on O-BDD electrode in neutral to alkaline media. This can be connected to the increased attraction of the cationic species present during electrooxidation of terconazole to the partially negatively charged O-BDD surface bearing even dissociated carboxylic groups. Although simultaneously the fact that the electrode operates at highly positive potential must be taken in consideration, the effect of partially negative charge is significant because the other BDD surfaces (H-, polished) do not exhibit distinctive second oxidation signals underlining the importance of electric interactions between the positively charged analytes/reaction intermediates and oxygen-containing groups on O-BDD surface. The E_p *vs.* pH dependences show a clear intersection of the linear parts only for this surface, at pH 4 and 9, *i.e.* around expected pK_a values of the distal and proximal nitrogen of piperazine ring. At the potential of *ca* +1.15 V, the oxidation presumably occurs again at the proximal nitrogen, forming a radical cation **6** stabilized on the conjugated benzene ring (see Scheme 1). This oxidation step was proved for structurally similar compounds containing an aromatic ring attached to the proximal nitrogen and possessing distal nitrogen blocked for imine formation [42].

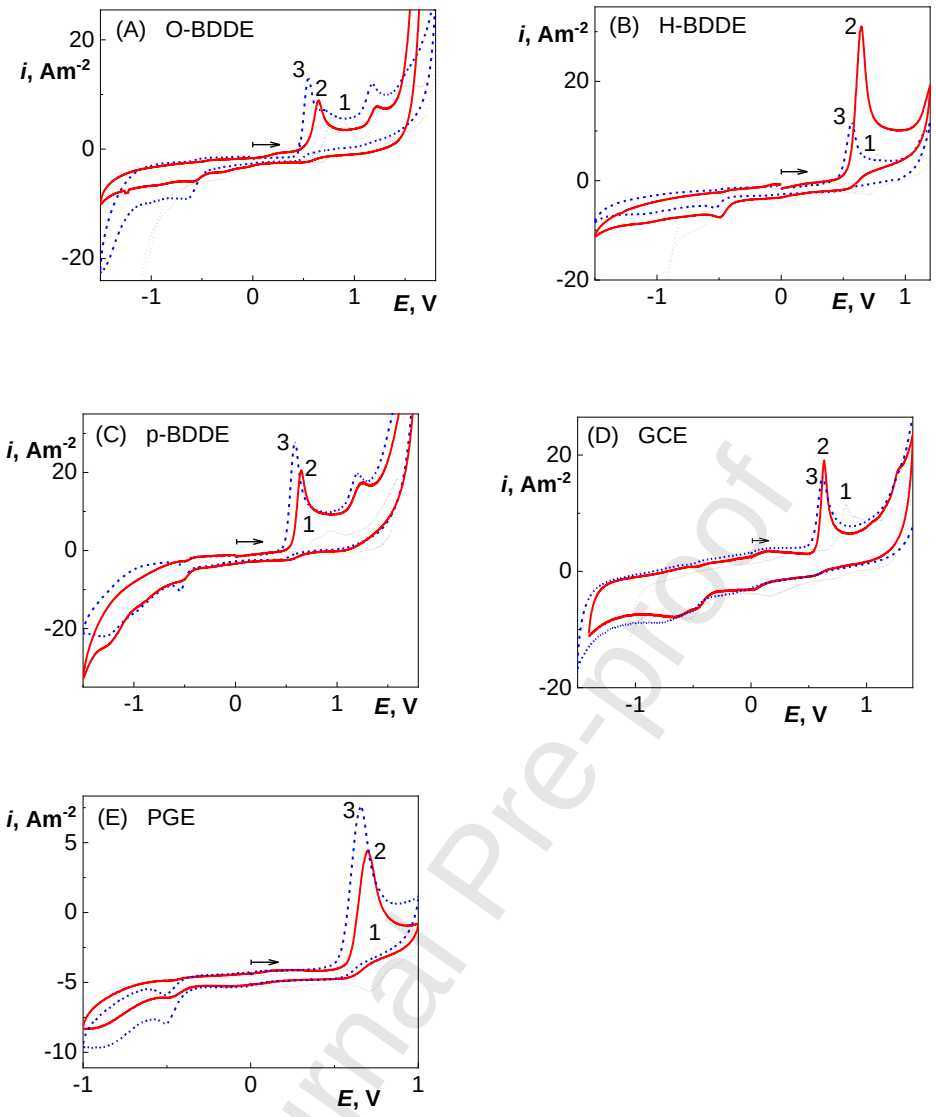

Fig. 1 Cyclic voltammograms of $1 \cdot 10^{-4}$ mol L^{-1} terconazole on (A) O-BDDE, (B) H-BDDE, (C) p-BDDE, (D) GCE, (E) PGE. Supporting electrolytes: (1; black dotted line) 0.1 mol L^{-1} phosphate buffer pH 2.3; (2; red full line) 0.1 mol L^{-1} phosphate buffer pH 7.2; (3; blue dashed line) 0.1 mol L^{-1} borate buffer pH 9.3. Scan rate 100 mV s^{-1}, started by anodic scan at 0 V.

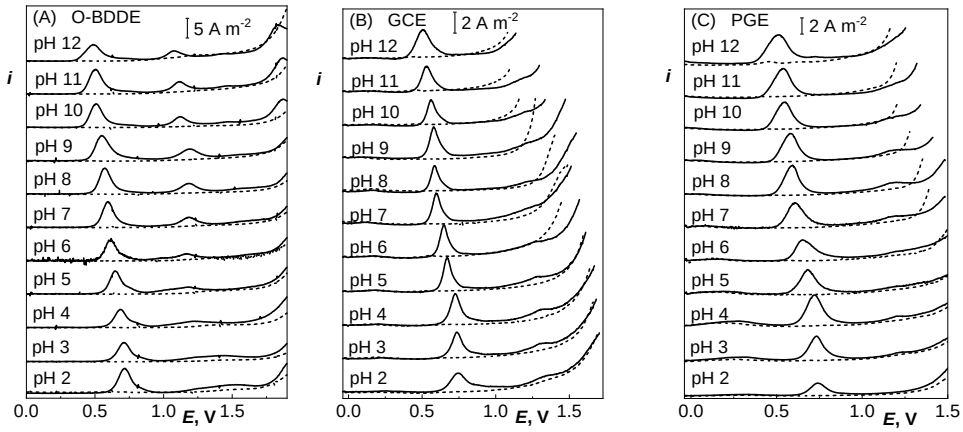

Fig. 2 DP voltammograms of $1 \cdot 10^{-4}$ mol L^{-1} terconazole on (A) O-BDDE, (B) GCE, and (C) PGE in BR buffer pH 2.0 – 12.0. Dotted lines represent supporting electrolytes.

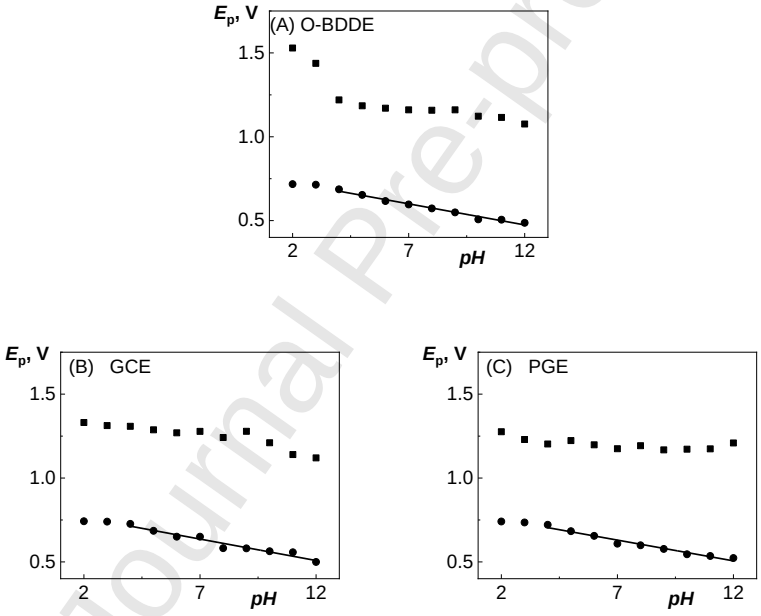

Fig. 3 Dependence of the peak potential E_p of $1 \cdot 10^{-4}$ mol L^{-1} terconazole on pH of BR buffer on (A) O-BDDE, (B) GCE, and (C) PGE (circles for the first; squares for the second anodic peak) measured by DPV.

Further, cyclic voltammograms are characterized by the presence of reduction signals in the reverse cathodic scan at the potential of *ca* 0 V to −0.6 V. Fig. 4 shows that these cathodic processes are associated with preceding oxidation processes, as the respective signal appears at the CVs only when the positive vertex potential is set just after the first oxidation peak (Fig. 4, curve B) and remains rather unchanged when the scan is reversed after the second oxidation peak. Thus, the cathodic process is presumably associated with reduction of compound **5**. The mechanism is questionable, nevertheless one-electron reductive cleavage of the bond between the proximal nitrogen and the benzene ring leading to piperazine and benzyl radical-type triazole derivative is probable, similarly as described for sodium 4-(3-methoxyphenyl)piperazine-1-carbodithioate (SMPC) containing structurally related moiety [42]. Terconazole itself is not reducible within the potential window of the studied carbon-based electrodes, as presented in 0.1 mol L^{-1} phosphate buffer pH 7.2 for O-BDD: no cathodic peak appears unless terconazole is oxidized first (Figure 4, curve C). This confirms different electrochemical behavior of the piperazine moiety, conjugated or standing alone, as the latter form is reducible at −0.67 V as presented in Fig. S1, while the former is inactive in a variety of compounds including azole agents summarized in Table 1. For some of them, appearance of cathodic signals was reported, but different moieties were supposed to be reduced, *e.g.* the carbonyl group of triazolone moiety in itraconazole [52] or carbonyl group of the terminal acid amide group of ketoconazole [33, 34].

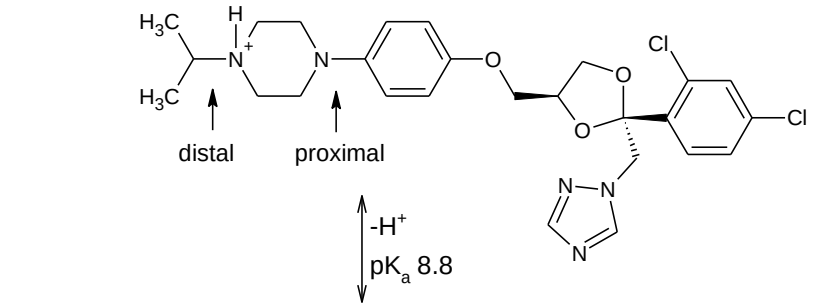

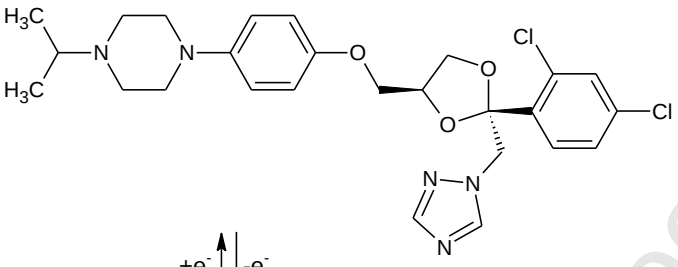

1

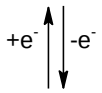

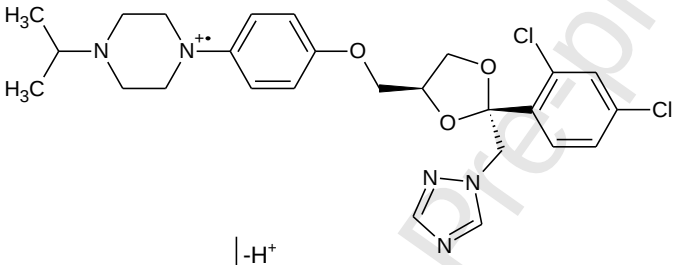

2

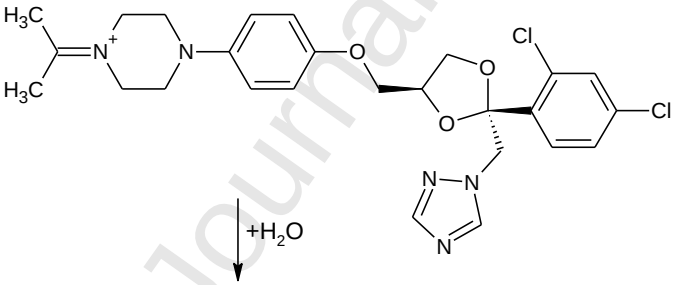

3

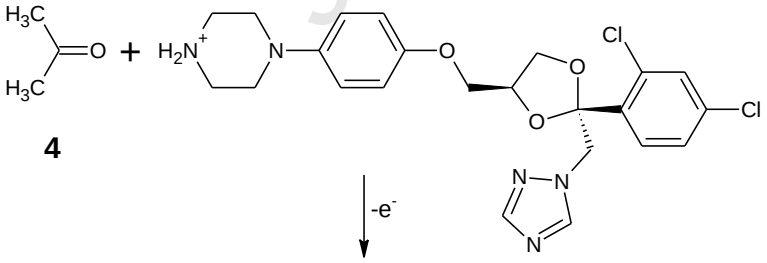

4

5

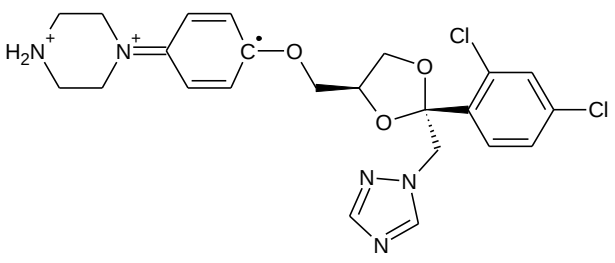

6

Scheme 1 Proposed mechanism of electrochemical oxidation of terconazole on carbon electrodes.

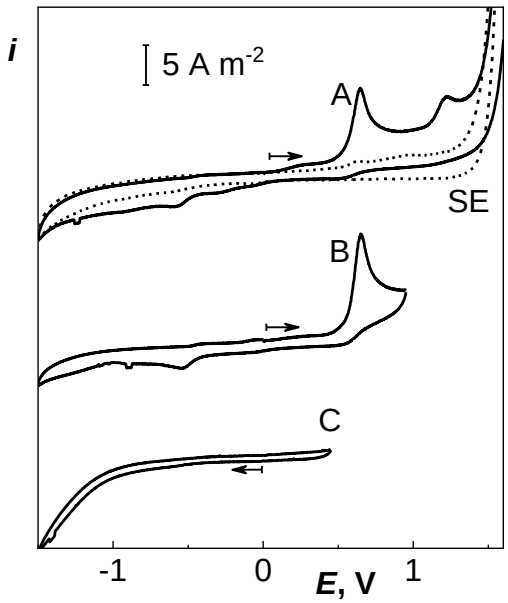

Fig. 4 Cyclic voltammograms of $1 \cdot 10^{-4}$ mol L^{-1} terconazole on O-BDDE in 0.1 mol L^{-1} phosphate buffer pH 7.2. Measured in potential range: (A) −1.50 V to +1.80 V (dotted line represents supporting electrolyte) (B) from −1.50 V to +0.95 V, (C) and from +0.45 V to −1.50 V. Scan rate 100 mV s^{-1}.

3.2. Optimization of voltammetric techniques and concentration dependences

Differential pulse voltammetry was used for quantitation of terconazole on O-BDD, PGE and GCE, using optimized electrode conditioning protocols, in 0.1 mol L^{-1} phosphate buffer pH 7.2. While renewal of GCE and PGE surface must be performed *ex-situ* using polishing by alumina and surface renewal using adhesion tape, respectively, O-BDD has the advantage of *in-situ* activation directly in the analyzed solution. Remarkable fouling of O-BDD surface characterized by peak height decrease by about 70 % was observed during five consecutive scans with the highest drop between the first and second scan (57 %), when no activation procedure was applied prior each scan. The successful strategy of surface conditioning entails the application of +2.4 V for 5 seconds while stirring, followed by 5 s of stabilization of the solution prior to scan. Absence of stabilization break leads to decreased repeatability of peak heights. Relative standard deviation (RSD) of peak heights ($c = 1 \cdot 10^{-4}$ mol L^{-1}) calculated for repeated DP voltammograms using this procedure is 1.1 %. The same protocol omitting the insertion of the positive potential resulted in RSD of 1.8 %. Nevertheless, the first recorded

curve was higher in comparison with the others, which would lead to complications when evaluating the analytical performance of the O-BDD electrode. This low RSD values widely outperform values obtained at GCE (4.6 %) and PGE (4.0 %); nevertheless, even these are acceptable if accepting the necessity of *ex-situ* regeneration of the surface of these electrodes.

Concentration dependences were measured using optimized protocols in 0.1 mol L^{-1} phosphate buffer pH 7.2. While for O-BDD they were evaluated for both anodic peaks, for GCE and PGE only the first one was taken into consideration as the second signal on these electrodes was rather indistinctive. Parameters of obtained calibration dependences are summarized in Table 2. On O-BDD, two linear ranges were obtained for both peaks, one for concentration range from 0.2 to 4 μmol L^{-1}, and the other for higher concentrations, from 4 to 100 μmol L^{-1}. The corresponding voltammograms and concentration dependences depicted in Fig. 5 clearly demonstrate the possibility of detection of terconazole in submicromolar range on O-BDD with detection limit of 0.40 μmol L^{-1}. The other tested electrode materials exhibited comparable (GCE, 0.50 μmol L^{-1}) or higher (PGE, 1.23 μmol L^{-1}) detection limits. Both sp^2 carbon electrodes required *ex-situ* polishing of the surface. An advantage of GCE was linearity of concentration dependence within the whole range from 1 to 100 μmol L^{-1}.

The mentioned L_D values cannot be directly compared with other electroanalytical techniques, as no other reports were found in the literature. Voltammetric methods for structurally related piperazine-based azolic agents, summarized in Table 1, exhibit comparable or higher L_D values for approaches based on reduction on mercury-based electrodes [33,34]. Methods based on the oxidation process usually resulted in lower L_Ds in 10^{-8} mol L^{-1} concentration range; nevertheless, it should be mentioned that they take advantage from the very strong adsorption of the azolic agents on the sp^2 carbon electrode surfaces, which is not the case of terconazole with redox process controlled by diffusion instead. BDD electrode (presumably in O-terminated mode according to given data) was used only for determination of ketoconazole with diffusion-controlled redox reaction and experimental detection limit of 0.30 μmol L^{-1} [22] was reached. Thus, similar analytical performance was found in our study for terconazole, holding the advantage of *in-situ* activation procedure.

Comparison of the presented electroanalytical with other analytical techniques favors the former approach. UV detection coupled to HPLC [7] or micellar liquid chromatography [8] resulted in L_Ds in 10^{-6} mol L^{-1} concentration range, similarly as first order derivative

spectrophotometry [7]. Comparable L_D in 10^{-7} mol L^{-1} concentration range was obtained for UHPLC with photodiode array detector [9].

Table 2

Parameters of concentration dependences and limits of detection, L_D, of terconazole obtained by DP voltammetry in 0.1 mol L^{-1} phosphate buffer pH 7.2 on O-BDDE, GCE and PGE.

Electrode	Linear dynamic range [μmol L^{-1}]	Slope [nA L μmol^{-1}]	Intercept [nA]	R^2	L_D [μmol L^{-1}]
O-BDDE	0.2 – 4	144 ± 16.0	32 ± 19	0.988	0.40
(1st peak)	4 – 100	51.9 ± 0.9	436 ± 23	0.999	–
O-BDDE	1 – 4	36.7 ± 2.7	3.9 ± 4.6	0.995	0.87
(2nd peak)	4 – 100	17.2 ± 0.3	100 ± 4	0.999	–
GCE	1 – 100	23.8 ± 0.4	66 ± 4	0.999	0.50
PGE	1 – 10	73.4 ± 5.0	406 ± 30	0.991	1.23
	10 – 100	36.3 ± 3.2	1109 ± 227	0.989	–

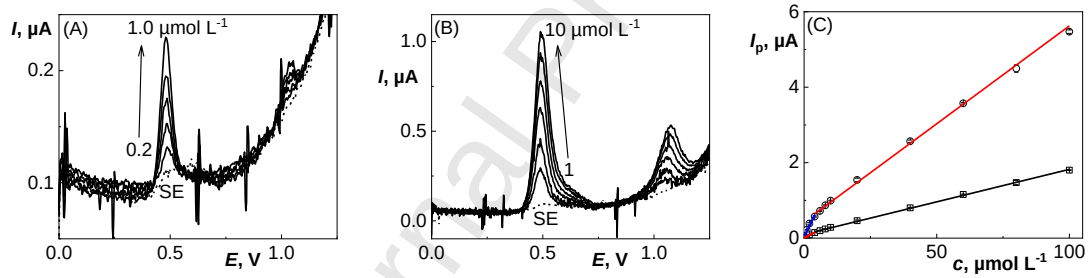

Fig. 5 DP voltammograms for (A) the lowest measurable concentration range 0.2, 0.4, 0.6, 0.8, and 1 μmol L^{-1} and (B) 1, 2, 4, 6, 8, and 10 μmol L^{-1}; (C) corresponding calibration dependences for terconazole in 0.1 mol L^{-1} phosphate buffer pH 7.2 measured on O-BDDE using *in-situ* activation at +2.4 V for 5 s prior each scan (○ – 1st anodic peak; □ – 2nd anodic peak). Error bars represent the 95 % confidence interval of the mean peak current (n=4), SE – supporting electrolyte.

Conclusion

In this study, the electrochemical behavior of terconazole was studied for the first time, using cyclic voltammetry and differential pulse voltammetry, on a variety of sp^2 and sp^3 carbon electrode materials including boron doped diamond electrode (BDD) with different surface treatment leading to O-terminated, H-terminated and polished surface, and on glassy carbon

and pyrolytic graphite electrodes. Measurements with all electrodes indicated similar behavior of terconazole, taking into consideration presence and potential positioning of voltammetric signals. The experiments confirmed similar interaction of terconazole and reaction intermediates with all tested surfaces, similar electron transfer kinetics and mechanism of the redox reactions. Terconazole is not directly reducible within the potential window on these electrode materials, thus our attention was paid to its oxidation in aqueous solutions in pH range from 2.0 to 12.0. Oxidation of terconazole proceeds in two steps leading to development of two anodic signals, the first one being well developed at potentials ranging from *ca* +0.55 V to +0.9 V, depending on the electrode used. An ECE mechanism was proposed for this signal, relying on oxidation of piperazine ring in the molecule, possessing two redox centers at the tertiary nitrogens. Different reaction pathways have been proposed for other azole agents possessing the piperazine moiety and other piperazine-based compounds. Nevertheless, the mechanisms are driven by the moieties bonded to the tertiary amines of piperazines as these influence their pK_a values, as well as stability of the reaction intermediates. More extended mechanistic studies including mass-spectrometric and NMR detection of products of electrochemical oxidation are needed to confirm the suggested mechanisms and to fully understand the effects of the structural motifs surrounding the piperazine ring.

The first anodic peak was used to optimize a DP voltammetric method for detection of terconazole in 0.1 mol L^{-1} phosphate buffer pH 7.2. The lowest detection limit of 0.40 μmol L^{-1} was achieved on O-terminated BDD, when *in-situ* anodic activation was used prior to each scan assuring repeatable peak heights (RSD 1.1 %). This is beneficial in comparison with GCE and PGE with the necessity of *ex-situ* polishing which worsens the signal repeatability (RSD ~ 4%) of the responses and detection limits.

This first study on electrochemical behaviour of terconazole clearly demonstrates the applicability of voltammetric methods or other electroanalytical approaches to its detection in various matrices of interest (e.g., pharmaceutical preparations, biological fluids) and demonstrates possibilities of carbon-based electrode materials which can be used for that purpose. The studies on the mechanism of redox reactions should be performed in a systematic way also for other piperazine-based biologically active agents to confirm structure of reaction (by)products, to evaluate the effect of the piperazine substituents, as well as to correlate the electrochemical reaction pathways with their biological activity.

Acknowledgements

The project was supported by the Czech Science Foundation (project 18-01710S) and carried out within the framework of Specific University Research (SVV 260440). Authors also thank the Regional Goverment of Castilla y León, Spain, and the EU-FEDER (CLU 2017-09).

References

[1] K. Walayat, N.A. Mohsin, S. Aslam, M. Ahmad, An insight into the therapeutic potential of piperazine-based anticancer agents. Turk. J. Chem., 43 (2019) 1-23. https://doi.org/10.3906/kim-1806-7.
[2] M. Locatelli, A. Kabir, D. Innosa, T. Lopatriello, K.G. Furton, A fabric phase sorptive extraction-High performance liquid chromatography-Photo diode array detection method for the determination of twelve azole antimicrobial drug residues in human plasma and urine, J. Chrom. B-Analyt. Technol. Biomed. Life Sci., 1040 (2017) 192-198. https://doi.org/10.1016/j.jchromb.2016.10.045.
[3] M.A. Pfaller, J. Riley, T. Koerner, Effect of terconazole and other azole antifungal agents on the sterol and carbohydrate-composition of *Candida albicans*, Diagn. Microbiol. Infect. Dis., 13 (1990) 31-35. https://doi.org/10.1016/0732-8893(90)90050-6.
[4] J.L. Thomason, Clinical evaluation of terconazole. United states experience, J. Reprod. Med., 34 (1989) 597-601.
[5] M. Castro-Puyana, A.L. Crego, M.L. Marina, Enantiomeric separation of ketoconazole and terconazole antifungals by electrokinetic chromatography: Rapid quantitative analysis of ketoconazole in pharmaceutical formulations, Electrophoresis, 26 (2005) 3960-3968. https://doi.org/10.1002/elps.200500100.
[6] M. Srilakshmi, S. A. Rahaman, K. Shanthakumari, Development And Validation Of UV-Spectrophotometric Method For The Estimation Of Terconazole In Bulk And Pharmaceutical Dosage Form, Indo Am. J. Pharm. Res., 3 (2013) 3057-3046. https://doi.org/10.1044/1980-iajpr.05180.
[7] R.I. Elbagary, E.F. Elkady, M.H. Tammam, A.A. Elmaaty, Simultaneous Estimation of Terconazole and Benzoic Acid in Bulk and Creams Using RP-HPLC, Derivative Spectrophotometry and Chemometric Techniques, J. Chem. Pharm. Res. 9 (2017) 280-291.
[8] M. Rizk, S.S. Toubar, M.M.A. El-Alamin, M.M.M. Azab, Micellar liquid chromatographic determination of sertaconazole and terconazole in bulk, pharmaceutical dosage forms and spiked human plasma, Bull. Fac. Pharm. Cairo University, 52 (2014) 155-164. https://doi.org/10.1016/j.bfopcu.2014.03.002.
[9] B.B. Chavan, G.L. Prasanna, P. Radhakrishnanand, E.R. Kosuri, P.D. Kalariya, M. Talluri, Development of a stability-indicating UPLC method for terconazole and characterization of the acidic and oxidative degradation products by UPLC-Q-TOF/MS/MS and NMR, New J. Chem., 42 (2018) 10761-10773. https://doi.org/10.1039/C8NJ00509E.
[10] R. Norkova, J. Jaklova Dytrtova, M. Jakl, D. Schroder, Formation of Tebuconazole Complexes with Cadmium(II) Investigated by Electrospray Ionization Mass Spectrometry, Water Air Soil Poll., 223 (2012) 2633-2640. https://doi.org/10.1007/s11270-011-1055-7.
[11] K. Novakova, T. Navratil, J. Jaklova Dytrtova, J. Chylkova, Application of Copper Solid Amalgam Electrode for Determination of Fungicide Tebuconazole, Int. J.. Electrochem. Sci., 8 (2013) 1-16.
[12] J.D. Lovic, D.Z. Mijin, M.B. Jovanovic, O.S. Glavaski, T.M. Zeremski, S.D. Petrovic, M.L.A. Ivic, An investigation of tebuconazole degradation using a gold electrode, C. R. Chim., 19 (2016) 639-645. https://doi.org/10.1016/j.crci.2016.01.014.

[13] J. Fischer, H. Dejmkova, J. Barek, Electrochemistry of Pesticides and its Analytical Applications, Curr. Org. Chem., 15 (2011) 2923-2935. https://doi.org/10.2174/138527211798357146.
[14] M. Moreno, E. Bermejo, A. Sanchez, M. Chicharro, A. Zapardiel, Application of matrix solid-phase dispersion to the determination of amitrole and urazole residues in apples by capillary electrophoresis with electrochemical detection, Anal. Bioanal. Chem., 391 (2008) 867-872. https://doi.org/10.1007/s00216-008-2058-0.
[15] A. Shah, A.H. Shah, N. Parveen, Z.U. Rehman, S.Z. Khan, U.A. Rana, S.U.D. Khan, J. Nisar, A. Lashin, R. Qureshi, Synthesis and electrochemical investigations of piperazines, Electrochim. Acta, 220 (2016) 705-711. https://doi.org/10.1016/j.electacta.2016.10.165.
[16] H. Knoth, G.K.E. Scriba, B. Buettner, Electrochemical behavior of the antifungal agents itraconazole, posaconazole and ketoconazole at a glassy carbon electrode, Pharmazie, 70 (2015) 374-378. https://doi.org/10.1691/ph.2015.4174.
[17] M. Shamsipur, K. Farhadi, Adsorptive stripping voltammetric determination of ketoconazole in pharmaceutical preparations and urine using carbon paste electrodes, Analyst, 125 (2000) 1639-1643. https://doi.org/10.1039/B001452O.
[18] T.Z. Peng, Q. Cheng, C.F. Yang, Adsorptive behavior and electrochemical determination of the anti-fungal agent ketoconazole, Fresenius J. Anal. Chem., 370 (2001) 1082-1086. https://doi.org/10.1007/s002160100773.
[19] K. Mielech-Lukasiewicz, H. Puzanowska-Tarasiewicz, A. Niedzielko, Electrooxidation of Some Antifungal Agents and Their Square-Wave Voltammetric Determination in Cosmetics and Pharmaceutics, Anal. Lett., 44 (2011) 955-967. https://doi.org/10.1080/00032719.2010.506934.
[20] J. Borowiec, L.L. Wei, L.H. Zhu, J.D. Zhang, Multi-walled carbon nanotubes modified glassy carbon electrode for sensitive determination of ketoconazole, Anal. Methods, 4 (2012) 444-448. https://doi.org/10.1039/C2AY05615A.
[21] A. Shalaby, W.S. Hassan, H.A.M. Hendawy, A.M. Ibrahim, Electrochemical oxidation behavior of itraconazole at different electrodes and its anodic stripping determination in pharmaceuticals and biological fluids, J. Electroanal. Chem., 763 (2016) 51-62. https://doi.org/10.1016/j.jelechem.2015.12.047.
[22] K. Mielech-Lukasiewicz, K. Roginska, Voltammetric determination of antifungal agents in pharmaceuticals and cosmetics using boron-doped diamond electrodes, Anal. Methods., 6 (2014) 7912-7922. https://doi.org/10.1039/C4AY01421A.
[23] S. Baluchová, A. Taylor, V. Mortet, S. Sedlaková, L. Klimša, J. Kopeček, O. Hák, K. Schwarzová-Pecková, Porous boron doped diamond films for dopamine sensing: Effect of boron doping level on morphology and electrochemical performance, Electrochim. Acta, 327 (2019) 135025. https://doi.org/10.1016/j.electacta.2019.135025.
[24] N.J. Yang, S.Y. Yu, J.V. Macpherson, Y. Einaga, H.Y. Zhao, G.H. Zhao, G.M. Swain, X. Jiang, Conductive diamond: synthesis, properties, and electrochemical applications, Chem. Soc. Rev., 48 (2019) 157-204. https://doi.org/10.1039/C7CS00757D.
[25] H. Glorian, V. Schmalz, P. Lochyński, P. Fremdling, H. Börnick, E.Worch, T. Dittmar, Portable analyzer for on-site determination of dissolved organic carbon. Development and field testing, Int. J. Environ. Res. Public Health, 15 (2018) 2335. https://doi.org/10.3390/ijerph15112335
[26] L.A. Hutton, J.G. Iacobini, E. Bitziou, R.B. Channon, M.E. Newton, J.V. Macpherson, Examination of the Factors Affecting the Electrochemical Performance of Oxygen-Terminated Polycrystalline Boron-Doped Diamond Electrodes, Anal. Chem., 85 (2013) 7230-7240. https://doi.org/10.1021/ac401042t.
[27] K. Schwarzova-Peckova, J. Vosahlova, J. Barek, I. Sloufova, E. Pavlova, V. Petrak, J. Zavazalova, Influence of boron content on the morphological, spectral, and electroanalytical

characteristics of anodically oxidized boron-doped diamond electrodes, Electrochim. Acta, 243 (2017) 170-182. https://doi.org/10.1016/j.electacta.2017.05.006.
[28] H.B. Suffredini, V.A. Pedrosa, L. Codognoto, S.A.S. Machado, R.C. Rocha-Filho, L.A. Avaca, Enhanced electrochemical response of boron-doped diamond electrodes brought on by a cathodic surface pre-treatment, Electrochim. Acta, 49 (2004) 4021-4026. https://doi.org/10.1016/j.electacta.2004.01.082.
[29] M. Brycht, K. Kaczmarska, B. Uslu, S.A. Ozkan, S. Skrzypek, Sensitive determination of anticancer drug imatinib in spiked human urine samples by differential pulse voltammetry on anodically pretreated boron-doped diamond electrode, Diam. Relat. Mater., 68 (2016) 13-22. https://doi.org/10.1016/j.diamond.2016.05.007.
[30] B. Uslu, B.D. Topal, S.A. Ozkan, Electroanalytical investigation and determination of pefloxacin in pharmaceuticals and serum at boron-doped diamond and glassy carbon electrodes, Talanta, 74 (2008) 1191-1200. https://doi.org/10.1016/j.talanta.2007.08.023.
[31] J. Spacek, A. Danhel, S. Hason, M. Fojta, Label-free detection of canonical DNA bases, uracil and 5-methylcytosine in DNA oligonucleotides using linear sweep voltammetry at a pyrolytic graphite electrode, Electrochem. Commun., 82 (2017) 34-38. https://doi.org/10.1016/j.elecom.2017.07.013.
[32] R.L. McCreery, Advanced carbon electrode materials for molecular electrochemistry, Chem. Rev., 108 (2008) 2646-2687. https://doi.org/10.1021/cr068076m.
[33] H. Knoth, T. Petry, P. Gartner, Differential pulse polarographic investigation of the antifungal drugs itraconazole, ketoconazole, fluconazole and voriconazole using a dropping mercury electrode, Pharmazie, 67 (2012) 987-990. https://doi.org/10.1691/ph.2012.2004.
[34] A.N.D. Dantas, D. De Souza, J.E.S. de Lima, P. de Lima-Neto, A.N. Correia, Voltammetric determination of ketoconazole using a polished silver solid amalgam electrode, Electrochim. Acta, 55 (2010) 9083-9089. https://doi.org/10.1016/j.electacta.2010.08.026.
[35] E. Fortin, J. Chane-Tune, P. Mailley, S. Szunerits, B. Marcus, J.P. Petit, M. Mermoux, E. Vieil, Nucleosides and ODN electrochemical detection onto boron doped diamond electrodes, Bioelectrochemistry, 63 (2004) 303-306. https://doi.org/10.1016/j.bioelechem.2003.10.027.
[36] A.N. Patel, S.Y. Tan, T.S. Miller, J.V. Macpherson, P.R. Unwin, Comparison and Reappraisal of Carbon Electrodes for the Voltammetric Detection of Dopamine, Anal. Chem., 85 (2013) 11755-11764. https://doi.org/10.1021/ac401969q.
[37] S. Baluchová, A. Daňhel, H. Dejmková, V. Ostatná, M. Fojta, K. Schwarzová-Pecková, Recent progress in the applications of boron doped diamond electrodes in electroanalysis of organic compounds and biomolecules – A review, Anal. Chim. Acta, 1077 (2019) 30-66. https://doi.org/10.1016/j.aca.2019.05.041.
[38] A.J. Bard, L.R. Faulkner, Electrochemical Methods, Fundamentals and Applications, Wiley, New York, 2004.
[39] R. Guidelli, R.G. Compton, J.M. Feliu, E. Gileadi, J. Lipkowski, W. Schmickler, S. Trasatti, Defining the transfer coefficient in electrochemistry: An assessment (IUPAC Technical Report), Pure Appl. Chem., 86 (2014) 245-258. https://doi.org/10.1515/pac-2014-5026.
[40] J.M. Kauffmann, J.C. Vire, G.J. Patriarche, L.J. Nunezvergara, J.A. Squella, Voltammetric oxidation of trazodone, Electrochim. Acta, 32 (1987) 1159-1162. https://doi.org/10.1016/0013-4686(87)80028-2.
[41] R.N. Hegde, N.P. Shetti, S.T. Nandibewoor, Electro-oxidation and determination of trazodone at multi-walled carbon nanotube-modified glassy carbon electrode, Talanta, 79 (2009) 361-368. https://doi.org/10.1016/j.talanta.2009.03.064.
[42] N. Parveen, A. Shah, S.Z. Khan, S.U.D. Khan, U.A. Rana, F. Fathi, A.H. Shah, M.N. Ashiq, A. Rauf, R. Qureshi, Z.U. Rehman, H.B. Kraatz, Synthesis, Spectroscopic Characterization, pH Dependent Electrochemistry and Computational Studies of Piperazinic

Compounds, J. Electrochem. Soc., 162 (2015) H32-H39. https://doi.org/10.1149/2.0761501jes.
[43] B. Uslu, B. Dogan, S.A. Ozkan, H.Y. Aboul-Enein, Electrochemical behavior of vardenafil on glassy carbon electrode: Determination in tablets and human serum, Anal. Chim. Acta, 552 (2005) 127-134. https://doi.org/10.1016/j.aca.2005.07.040.
[44] D. Perrin, Dissociation Constants of Organic Bases in Aqueous Solution. IUPAC Chemical Data Series: Supplement, Buttersworth, London, 1972.
[45] F. Khalili, A. Henni, A.L.L. East, pK(a) Values of Some Piperazines at (298, 303, 313, and 323) K, J. Chem. Eng. Data, 54 (2009) 2914-2917. https://doi.org/10.1021/je900005c.
[46] C.J. Shoemaker, K.L. Schornberg, S.E. Delos, C. Scully, H. Pajouhesh, G.G. Olinger, L.M. Johansen, J.M. White, Multiple Cationic Amphiphiles Induce a Niemann-Pick C Phenotype and Inhibit Ebola Virus Entry and Infection, Plos One, 8 (2013) e56265. https://doi.org/10.1371/journal.pone.0056265.
[47] Janssen Inc., Terazol - terconazole vaginal cream, https://pdf.hres.ca/dpd_pm/00026484.pdf, downloaded 1.12.2019.
[48] R. Courtney, D. Wexler, E. Radwanski, J. Lim, M. Laughlin, Effect of food on the relative bioavailability of two oral formulations of posaconazole in healthy adults, Br. J. Clin. Pharmacol., 57 (2004) 218-222. https://doi.org/10.1046/j.1365-2125.2003.01977.x.
[49] M. Skiba, M. Skiba-Lahiani, H. Marchais, R. Duclos, P. Arnaud, Stability assessment of ketoconazole in aqueous formulations, Int. J. Pharm., 198 (2000) 1-6. https://doi.org/10.1016/S0378-5173(99)00279-3.
[50] R. Baran, Essentials of Heterocyclic Chemistry I, https://www.scripps.edu/baran/heterocycles/Essentials1-2009.pdf, downloaded 25.11.2019.
[51] S.A. Ozkan, B. Dogan, B. Uslu, Voltammetric analysis of the novel atypical antipsychotic drug quetiapine in human serum and urine, Microchim. Acta, 153 (2006) 27-35. https://doi.org/10.1007/s00604-005-0457-x.
[52] P. Arranz, A. Arranz, J.M. Moreda, A. Cid, J.F. Arranz, Stripping voltammetric and polarographic techniques for the determination of anti-fungal ketoconazole on the mercury electrode, J. Pharmaceut. Biomed. Anal., 33 (2003) 589-596. https://doi.org/10.1016/s0731-7085(03)00247-4.

Declaration of competing interests

☒ The authors declare that they have no known competing financial interests or personal relationships that could have appeared to influence the work reported in this paper.

☐The authors declare the following financial interests/personal relationships which may be considered as potential competing interests:

Author Statement

JAN FISCHER: data acquisition, methodology, writing original draft; JAVIER GONZÁLEZ-MARTÍN: investigation, data acquisition; PAWEL LOCHYŃSKI: formal analysis, review; HANA DEJMKOVÁ: data curation, formal analysis, writing original draft; KAROLINA SCHWARZOVÁ-PECKOVÁ: conceptualization, funding acquisition, validation, writing, review and editing; MARISOL VEGA: conceptualization, funding acquisition, writing, review and editing.

Graphical abstract

Highlights

- The first electrochemical study of terconazole using voltammetric techniques is described.
- Glassy carbon, pyrolytic graphite and oxygen-, hydrogen- and polished boron doped diamond (BDD) electrode were employed
- Terconazole gives well developed pH-dependent signals in cyclic voltammetry at *ca* +0.5 – 0.8 V due to oxidation of piperazine moiety
- Terconazole is not reducible within the potential window of tested electrode materials
- The lowest detection limit of 0.40 μmol L^{-1} was achieved on O-terminated BDD using *in-situ* anodic activation